SCIENCE CHINA
Earth Sciences

•RESEARCH PAPER•

August 2020 Vol.63 No.8: 1161–1175
https://doi.org/10.1007/s11430-019-9576-x

A continuous simulation of Holocene effective moisture change represented by variability of virtual lake level in East and Central Asia

Yu LI*, Yuxin ZHANG, Xinzhong ZHANG, Wangting YE, Lingmei XU, Qin HAN, Yichan LI, Hebin LIU & Simin PENG

Key Laboratory of Western China's Environmental Systems (Ministry of Education), College of Earth and Environmental Sciences, Center for Hydrologic Cycle and Water Resources in Arid Region, Lanzhou University, Lanzhou 730000, China

Received June 1, 2019; revised December 7, 2019; accepted January 8, 2020; published online April 1, 2020

Abstract The fluctuation of a single lake level is a comprehensive reflection of water balance within the basin, while the regional consistent fluctuations of lake level can indicate the change of regional effective moisture. Previous researches were mainly focused on reconstructing effective moisture by multiproxy analyses of lake sediments. We carried out a series of experiments, including a transient climate evolution model, a lake energy balance model and a lake water balance model to simulate continuous Holocene effective moisture change represented by variability of virtual lake level in East and Central Asia. The virtual lake level, area, water depth and salinity are not equivalent to actual values, but we estimated relative changes of the regional effective moisture. We also explored the driving mechanisms of effective moisture change in different geographical regions. Our results indicated that gradually falling effective moisture during the Holocene in northern China was due to the combined effects of high lake evaporation caused by longwave and shortwave radiation, and low precipitation caused by reductions of summer solar insolation. A decline in effective moisture through the Holocene in the Tibetan Plateau and southern Central Asia resulted from decreased precipitation because of the weakening of the Asian summer monsoon. Increased precipitation induced by the strengthening of the westerly circulation contributed to the effective moisture rise during the Holocene in northern Central Asia.

Keywords Effective moisture, Virtual lake level, Continuous simulation, Holocene, Solar radiation

Citation: Li Y, Zhang Y, Zhang X, Ye W, Xu L, Han Q, Li Y, Liu H, Peng S. 2020. A continuous simulation of Holocene effective moisture change represented by variability of virtual lake level in East and Central Asia. Science China Earth Sciences, 63: 1161–1175, https://doi.org/10.1007/s11430-019-9576-x

1. Introduction

Lake level records are important indicators of regional and global environmental change (Chen et al., 2003; Xiao et al., 2004; Shen, 2013; Zhang et al., 2016; Zheng et al., 2018). Studying the lake evolution and environmental change during the Holocene is of great significance for predicting the future global climate change (Innes, 1991; Davis et al., 2000). In recent decades, researches on the climate change of Hulun lake (Wen et al., 2010; Zhang et al., 2018), Qinghai lake (Madsen et al., 2008; Li et al., 2018), Erhai lake (Shen et al., 2005b), Issyk-Kul (Ricketts et al., 2001), Bosten lake (Wünnemann et al., 2006; Yao et al., 2018), and Aral Sea (Boomer et al., 2000; Sharma et al., 2018) have attracted extensive attention from scientists. The preceding studies suggested that lake level variations document changes in regional effective moisture because they reflect the lake's hydrologic balance (Qin and Yu, 1998; Anderson et al., 2005, 2011; Luoto and Sarmaja-Korjonen, 2011). Lake water balance system has complicated processes with many restrictive

* Corresponding author (email: liyu@lzu.edu.cn)

climatic factors. Relevant researches were mostly focused on reconstructions of lake level, regional effective moisture and paleoenvironment using geomorphic, sedimentological, and biostratigraphic methods. However, with the development of paleoclimatology, only using lake sediments as indicators to reconstruct lake evolution, water balance fluctuation and paleoenvironment change cannot more specifically explain the mechanism of paleoclimate change. Therefore, it is necessary to quantitatively reconstruct and simulate the lake's hydrologic balance from a new perspective.

Lake level fluctuations are primarily caused by changes in on-lake precipitation, lake evaporation and runoff from the drainage basin, and these fluxes are governed by many climatic and hydrologic processes. The energy balance and water balance models are widely used in many researches which are devoted to reconstructing the water balance fluctuations of a lake (Morrill, 2004; Li and Morrill, 2010, 2013; Li and Liu, 2016). Qin and Yu (1998) successfully explained the distribution pattern of lake level during the Last Glacial Maximum in East and Central Asia by introducing physical quantities (precipitation minus evaporation). Likewise, Li and Morrill (2010) revealed that lake surface evaporation, which was likely decreased during the Last Glacial Maximum, plays a significant role in the lake water balance. Xue and Yu (2010) analyzed the overall pattern of effective precipitation and atmospheric circulation in three periods, including 30, 18 and 6 kyr BP, and concluded that the change of lake level in these three characteristic periods was mainly controlled by the influence of atmospheric circulation.

Transient Climate Evolution Experiment (TraCE-21 kyr), as a new attempt in paleoclimate simulation, is able to simulate the paleoclimate process continuously since the Last Glacial Maximum (He et al., 2013; Cheng et al., 2014). We used a series of models, a TraCE-21 kyr model, a lake energy balance model and a lake water balance model to perform a continuous simulation of hypothetical lake level change for tracking the variability of regional effective moisture during the Holocene in East and Central Asia. Furthermore, we combined simulated results with the paleoenvironmental indicators such as stable isotope $\delta^{13}C$, $\delta^{18}O$, total organic carbon (TOC), total nitrogen (TN), and carbon nitrogen ratio (C/N) to verify the relationship between regional virtual lake level change and climate variation. Lastly, trend analysis and Empirical Orthogonal Function (EOF) are performed on meteorological elements which can directly reflect climate processes, for further exploring the possible mechanisms of virtual lake level and effective moisture changes.

Lake water balance system is constantly responding to changes of climatic conditions on different time scales. On the millennial scale, the lake level variation and temperature have a certain relationship with the regional atmospheric circulation, while they have seasonal characteristics on the interannual scale. A lake's water level depends on its water balance, and temperature is related to its energy balance. Accordingly, whether on a global or regional scale, the hydrological and energy conditions of lakes represent their responses to changes in energy and water of the climate system. Our goal is not to simulate an actual lake level change, but to assume that each land grid cell is a separate lake. It should be noted that this study is not to simulate the specific lake surface energy and water balance process in East and Central Asia but to complete a sensitivity study of regional effective moisture to climate change. Comparing paleoclimate simulation results with paleoclimate records, the authenticity and accuracy of the simulation results can be verified. Meanwhile, the indication significance of paleoclimatic records can be explored based on the simulation results. We aim to use information about the cause of water balance fluctuation to improve the climatic interpretation of East and Central Asia. In the context of global warming, the study of Holocene lake evolution and environmental change is particularly important to predict future climate change. Our findings provide a large amount of new evidence, which reflects the past climate change and mechanisms of regional effective moisture variability, as well as a new perspective to comprehensively understand regional effective moisture change since the Holocene.

2. Model descriptions

2.1 Transient climate evolution experiment

We used the National Center for Atmospheric Research's (NCAR) model—Transient Climate Evolution over the last 21000 years (TraCE-21 kyr) that is completed by the Community Climate System Model version 3 (CCSM 3), to simulate continuous effective moisture since the Holocene by building a virtual lake model. TraCE-21 kyr is a synchronously coupled atmosphere-ocean circulation model simulation and provides the four-dimensional model datasets. This project investigates the mechanisms and feedbacks of the coupled atmosphere-ocean-sea ice-land surface, which can explain the evolution of the climate system over the last 21000 years (He, 2011).

TraCE-21 kyr studies the climate evolution during the Last Glacial Maximum, and simulates several abrupt climate events, such as the surface climate experienced cooling during Heinrich Event 1 (19–14.7 kyr) in the North Atlantic region, an abrupt warming occurred at the onset of the Bølling-Allerød (14.7–12.9 kyr), and a short period of Younger Dryas cold phase (12.9–11.7 kyr), based on paleoclimatic proxy data (Yang et al., 2015). During the Last Glacial Maximum, proxy reconstructions of Atlantic Meridional Overturning Circulation (AMOC) from deep sediments provide evidence that the millennial-scale variability of AMOC is consistent with the climate evolution including

abrupt climate change events (Liu et al., 2009). Therefore, AMOC which is quite sensitive to the surface meltwater fluxes, is possible to carry out TraCE-21 kyr in CCSM 3 by adjusting the strength of AMOC and earth's orbital parameters (Stommel, 1961; Rahmstorf et al., 2005). On account of the insufficient knowledge of meltwater discharges, He (2011) conducted several experiments that have same original condition but different rates or locations of meltwater discharges during several abrupt climate change events.

The CCSM 3 is affected by the instantaneous greenhouse gas concentration and the orbital driven insolation changes in the entire process of TraCE simulation. The concentration records and radiative forcing from atmospheric carbon dioxide (CO_2), methane (CH_4), and nitrous oxide (N_2O) are from Joos and Spahni (2008). Astronomical values for precession, obliquity and eccentricity are set according to Berger (1978). The ICE-5G reconstruction is used to specify continental ice sheets for continuous simulation, and ice sheet area and height are set according to Peltier (2004). The melt-water forcing is set according to Liu et al. (2009) and He (2011), and the vegetation is prescribed to modern values.

2.2 Lake energy balance model

On the basis of the Hostetler and Bartlein's model (Hostetler and Bartlein, 1990), one-dimensional lake energy balance model was applied to calculate virtual lake evaporation for all model grid cells between 60°E–140°E and 10°N–60°N in land. Morrill (2004) calculated interannual variations in evaporation over the lake using lake energy balance model, as well as verified the feasibility of the model in Asia simulation. In this model, the energy balance of the lake surface is not only controlled by the evaporation but also other energies which include shortwave and longwave radiation absorbed by the water surface, longwave radiation emitted by the water surface and the sensible heat flux. When the water temperature is at the freezing point, the surface energy balance is negative, driving the ice forms. On the contrary, lake ice melts when the surface energy balance is positive.

For this model, energy fluxes mixing between the surface water and lower layers can be ignored because the simulated lake at each model grid cell is a hypothetical 1-meter deep, freshwater lake. Salinity has great influences on the saturation vapor pressure, so that increasing salinity will decrease evaporation according to empirical relationships in Dickson et al. (1965). Given that, the evaporation model conducts an experiment of increasing lake depth to 5 and 10 m and increasing lake salinity to 10 ppt, which shows only small changes occur in lake evaporation (1–2%). We emphasize that it is not our intent to simulate actual lakes in East and Central Asia, but to complete a sensitivity study of lake evaporation to climate conditions, which is similar to the approach of Hostetler and Small (1999), who discuss the use of hypothetical lakes for impact assessment. And the sensitivity tests of lake depth and salinity give us confidence that our calculations of lake evaporation are not lake-specific, but are applicable to many of the lakes that exist in this region. The lake surface energy balance is calculated as (Li and Morrill, 2010):

$$c_w \rho_w z \frac{\partial T}{\partial t} = \varphi_s + \varphi_{ld} - \varphi_{lu} \pm Q_e \pm Q_h, \tag{1}$$

where c_w is the specific heat of water (J kg^{-1} K^{-1}), ρ_w is the density of water (kg m^{-3}), z is the lake depth (m), T is the lake temperature (K), t is the time (s), φ_s is the shortwave radiation absorbed by the water surface, φ_{ld} is longwave radiation absorbed by the water surface, φ_{lu} is longwave radiation emitted by the water surface, Q_e is the latent heat flux, and Q_h is the sensible heat flux. Latent and sensible heat fluxes are calculated using the standard bulk aerodynamic formulations of Dickinson et al. (1993):

$$Q_e = L_v \rho_a C_D V_a (q_s - q_a), \tag{2}$$

$$Q_h = C_p \rho_a C_D V_a (T_s - T_a), \tag{3}$$

where the subscripts a and s refer to air and surface, respectively, L_v is the latent heat of vaporization, ρ_a is the density of air, V_a is wind speed, q is specific humidity, C_p is the specific heat of air, C_D, the momentum drag coefficient, is a function of the neutral drag coefficient which depends on the roughness length, and the surface bulk Richardson number which depends on the wind speed and the near-surface temperature gradient, and T is temperature. Vertical transfer of heat between layers in the lake (z=1 m) is accomplished through convective mixing and eddy and molecular diffusion. Schematic illustration of the models is described in Figure 1.

Input values from the TraCE-21 kyr database are: 2-m air temperature, surface temperature, 2-m wind speed, and shortwave and longwave radiation incident at the land surface. The time-step of the lake model is 30 min, but climate model output is continuous monthly data. By using function "interp 3" of matlab, we linearly interpolate between monthly-averaged TraCE-21 kyr outputs (m s^{-1}) to obtain input values for the lake energy-balance model at a 30-min time step (m s^{-1}). Linear interpolation is the technique of building a simple, continuous analytical model for the unknown physical quantity from the known data points, so that the characteristics of the unknown physical quantity can be inferred from the model. And the principle is that given the coordinates (x_0,y_0) and (x_1,y_1) to get the value of x on the line at some point in the interval $[x_0,x_1]$, which can be described as follows:

$$\frac{y-y_0}{x-x_0} = \frac{y_1-y_0}{x_1-x_0}. \tag{4}$$

Since we know the x value, we can get the y value from the

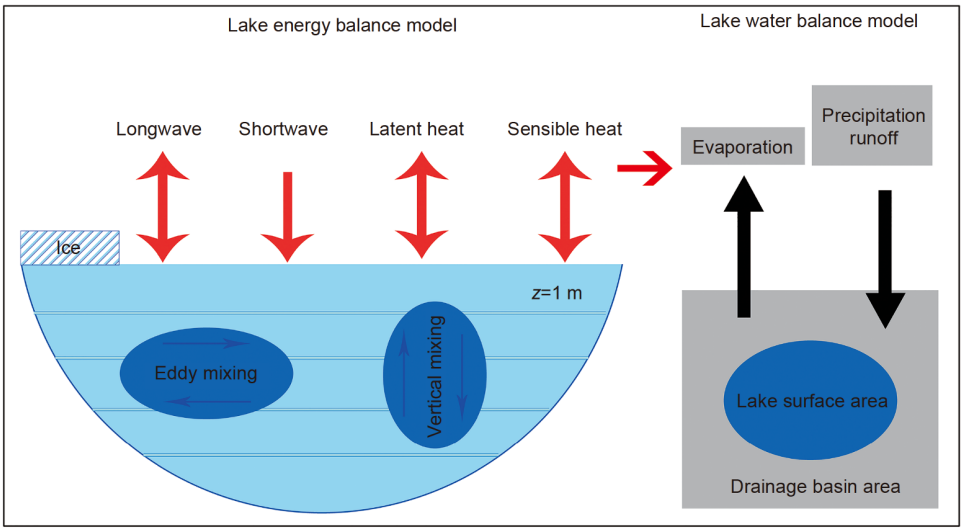

Figure 1 Schematic illustration of the lake energy and water balance models.

eq. (5):

$$y = y_0 + \frac{(x-x_0)y_1-(x-x_0)y_0}{x_1-x_0}. \quad (5)$$

Previous study from Morrill et al. (2001) showed that the amount of annual lake evaporation estimated from monthly data interpolated to a 30-min time step is accurate to within 3%, using modern meteorological measurements at hourly, daily or monthly resolutions. This is the case because the thermal inertia of lake prevents the lake surface evaporation from changing greatly with meteorological fluctuations on short scales (Pollard and Schulz, 1994). In the end, the TraCE-21 kyr output is integrated with the lake energy balance model to calculate the surface evaporation of the virtual lake, then calculate the average value of 50 years, as well as obtain the final results.

2.3 Lake water balance model

When calculating the hypothetical lake level, we assumed that the lake is in hydrological equilibrium with stable state during the process of climate change. This is a reasonable assumption, since the study takes into account that the lake has a shorter response process to climate change. The water balance of steady-state lake can be expressed as Li and Morrill (2013):

$$D = A_B R + A_L(P_L - E_L), \quad (6)$$

where D is discharge from the lake (m^3 $year^{-1}$), A_B is area of the drainage basin (m^2), R is runoff from the drainage basin (m $year^{-1}$), A_L is area of the lake (m^2), P_L is on-lake precipitation (m $year^{-1}$) and E_L is lake evaporation (m $year^{-1}$). On account of the requirement of A_B and A_L values, eq. (6) is not a generalized solution for a hypothetical lake, and the process of lake level change cannot be well calculated. Therefore, this equation is simplified for grid cells where $P_L-E_L\geq 0$ and grid cells where $P_L-E_L<0$. And we can obtain conclusions about the direction of virtual lake level change without providing lake-specific information, which is explained in the following two paragraphs.

Regardless of the values of A_B and A_L, lakes in grid cells where $P_L-E_L\geq 0$ must contain open lakes (i.e., $D>0$), adjust to water-balance changes by discharging more or less water. Eq. (6) manifests that, if the change in R and the change in P_L-E_L during the Holocene have different signs, the sign of the change in D will depend on A_B and A_L which are lake specific variables. For the grid cells with $P_L-E_L\geq 0$, we concluded that a change in the water balance, D, during the Holocene is positive (negative) when both the changes in R and P_L-E_L are positive (negative).

For lakes in grid cells where $P_L-E_L<0$, the net water loss from the lake surface must be compensated by runoff into the lake. These lakes adjust to water-balance changes through changes in the ratio of A_L to A_B, as described by setting $D=0$ in eq. (6):

$$\frac{A_L}{A_B} = \frac{R}{(E_L-P_L)}, \quad (7)$$

where A_L/A_B represents virtual lake level. Eq. (7) shows that, the ratio of A_L/A_B is not lake-specific for closed lakes (i.e., lakes with $D=0$) and is determined by climate (Benson and Paillet, 1989). Thus, for grid cells with $P_L-E_L<0$, we calculated A_L/A_B values and compared these values between simulations to determine relative changes in virtual lake level.

In order to determine the relative water balance change during the Holocene, we combined the values of P_L, E_L and R with eqs. (6) and (7). Then, we attributed the changes in the relative direction of water balance to evaporation, precipitation or both, and looked for which variables have

contributed effectively to changes in the net water balance. Since runoff (precipitation minus evaportranspiration) anomalies are highly correlated to precipitation anomalies, any productive contributions from runoff are counted as a contribution by precipitation. For our purpose, this study is not to simulate the specific lake surface energy and water balance process in East and Central Asia, instead, to use virtual lakes as a carrier to infer changes in regional effective moisture in the Holocene. Then based on the simulations of average regional effective moisture and hydroclimatic conditions, we discussed the driving mechanisms of regional climate change.

2.4 Mathematical modelling and calculation

To examine spatially and temporally variability of lake level, we chose to use the EOF method. It was introduced to meteorological and climatic research for the first time in 1950s, which is now widely used in other disciplines. This method has been detailed previously in many papers (Kundu and Allen, 1976; Weare and Newell, 1977). EOF is a method of analyzing the structural features in matrix data, and extracting the main data's feature vector. In general, the feature vector corresponds to a spatial sample, and the principal component corresponds to a time variation. The first principal component tends to characterize the average distribution of the original time series.

2.5 Selection of paleoclimate records

In this paper, paleoclimate records were summarized on the basis of following criteria: (1) the records come from lake deposits or lake geomorphological evidence; (2) records can cover most part of the Holocene period without interruption, and (3) the proxies derived from the records should indicate changes in lake level, effective moisture or hydrological climate.

3. Modeled virtual lake level and paleoclimate records

3.1 Verification of simulation results

According to the climatic similarities and topographic differentiation, we divided East and Central Asia into five regions: northern China, southern China, northern Central Asia, southern Central Asia, and Tibetan Plateau. Many lake records have been collected to validate simulation results (Figure 2a), and more details are prescribed in Table 1. Before considering model results, to review and summarize the large-scale patterns in lake level during the Holocene which we expect the models to simulate is important. These models must be able to reproduce these patterns if they are useful in testing hypotheses about the cause of lake level change. Both the tendency chart (Figure 2b) and time series (Figure 3) show that simulations indicate lake level fell through the Holocene in northern China, southern China (with the exception of coastal regions, where the late Holocene high lake level was maintained by high coastal precipitation, possibly resulted from changes in local ocean feedbacks), Tibetan Plateau and southern Central Asia, while lake level rose in northern Central Asia.

Most of the lake levels in northern China reach their highest level during the early Holocene, and then descend around the mid-Holocene (Table 1). This changing pattern has the similar trend with modeled virtual lake level (Figure 3a1), which indicates effective moisture in most northern China decreased from mid-Holocene to late Holocene. However, there are some differences, such as rising lake level in Hulun lake during 8–0 cal kyr BP. Lakes in southern China show the highest lake level around the early Holocene, intermediate lake level at the mid-Holocene and the lowest

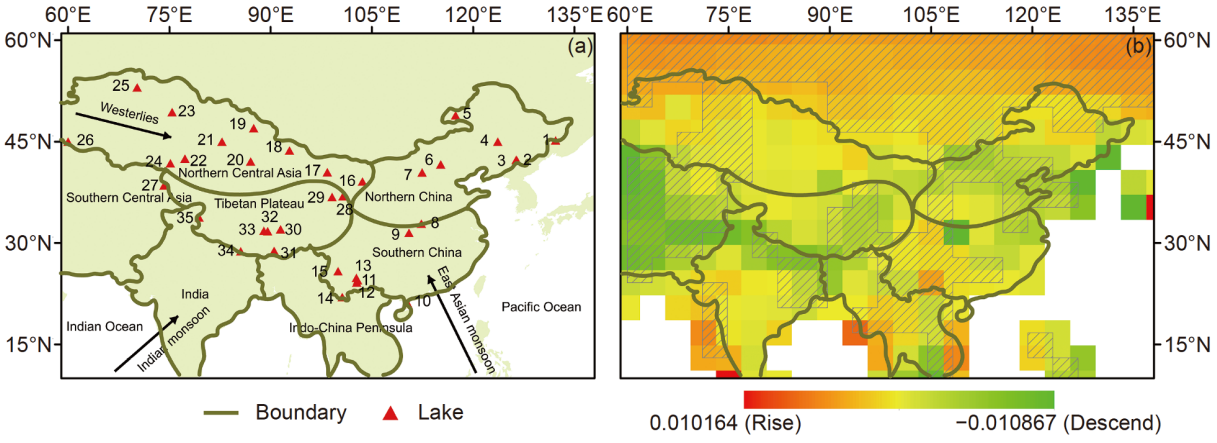

Figure 2 Lake sites selected in East and Central Asia, and dominant circulation systems of the westerlies, Indian monsoon, and East Asian monsoon (a) and trend analysis in lake level during the Holocene (b). Striping indicates the significance test is over 95%.

Table 1 Summary of lake level changes during the Holocene in East and Central Asia

Region	No.	Lake	Longitude	Latitude	Lake level fluctuations during the Holocene	References
Northern China	1	Xingkai lake	132.2°E	45.2°N	The lake level began to decline since the early Holocene	Wu and Shen (2010a, 2010b)
	2	Hani lake	126.5°E	42.2°N	The lake level began to decline since the early Holocene	Cui et al. (2006); Yu et al. (2008)
	3	Erlongwan Maar Lake	126.36°E	42.3°N	The lake level began to rise since the early Holocene	You and Liu (2012); Wang et al. (2012)
	4	Dabusu lake	123.65°E	45°N	The lake level began to rise in the early Holocene and then declined	Shen et al. (1998); Jie et al. (2001)
	5	Hulun lake	117.4°E	48.9°N	The lake level began to decline in the early Holocene and then rose	Wen et al. (2010); Xiao et al. (2009)
	6	Bayanchagan lake	115.21°E	41.65°N	The lake level began to rise in the early Holocene and then declined	Jiang et al. (2006)
	7	Daihai lake	112.45°E	40.45°N	The lake level began to rise in the early Holocene and then declined	Sun et al. (2009); Xiao et al. (2004)
Southern China	8	Longquan lake	112.33°E	32.87°N	The lake level began to rise in the early Holocene and then declined	Li and Yao (1993)
	9	Dajiu lake	110.5°E	31.5°N	The lake level began to decline since the early Holocene	Ma et al. (2008)
	10	Huguangyan Maar lake	110.28°E	21.15°N	The lake level began to decline since the early Holocene	Wu et al. (2012)
	11	Xingyun lake	102.88°E	24.5°N	The lake level began to decline since the early Holocene	Hodell et al. (1999)
	12	Qilu lake	102.75°E	24.17°N	The lake level began to decline in the early Holocene and then rose	Brenner et al. (1991)
	13	Dianchi lake	102.7°E	24.85°N	The lake level began to decline in the early Holocene and then rose	Zhang et al. (2009)
	14	Manxing lake	100.6°E	22°N	The lake level began to decline since the early Holocene	Tang (1992)
	15	Erhai lake	99.98°E	25.84°N	The lake level began to decline in the early Holocene and then rose	Zhou et al. (2003)
Northern Central Asia	16	Qingtu lake	103.6°E	39.1°N	The lake level began to rise in the early Holocene and then declined	Zhao et al. (2005)
	17	Huahai lake	98.4°E	40.5°N	The lake level began to decline since the early Holocene	Hu et al. (2003)
	18	Balikun lake	92.8°E	43.7°N	The lake level began to rise in the early Holocene and then declined	Zhao et al. (2015)
	19	Wulungu lake	87.5°E	47°N	The lake level began to decline in the early Holocene and then rose	Liu et al. (2008a)
	20	Bosten lake	87.05°E	42.08°N	The lake level began to decline in the early Holocene and then rose	Wünnemann et al. (2006)
	21	Aibi lake	82.8°E	45°N	The lake level began to decline since the early Holocene	Wang et al. (2013)
	22	Issyk-Kul	77.30°E	42.50°N	The lake level began to decline in the early Holocene and then rose	Ricketts et al. (2001); Ferronskii et al. (2003)
	23	Pashennoe	75.40°E	49.37°N	The lake level began to decline in the early Holocene and then rose	Tarasov and Kremenetskii (1995)
	24	Sonkel	75.15°E	41.82°N	The lake level began to decline in the early Holocene and then rose	Sevastyanov and Smirnova (1986)
	25	Karas'e	70.22°E	53.03°N	The lake level began to decline in the early Holocene and then rose	Tarasov and Kremenetskii (1995)
	26	Aral	60°E	45°N	The lake level began to rise in the early Holocene and then declined	Boomer et al. (2000)
Southern Central Asia	27	Rangkul-Shorkul	74.20°E	38.52°N	The lake level began to rise in the early Holocene and then declined	Sevastyanov and Dorofeyuk (1992)
Tibetan Plateau	28	Qinghai lake	100.7°E	36.9°N	The lake level began to rise in the early Holocene and then declined	Madsen et al. (2008)
	29	Chaka lake	99.1°E	36.8°N	The lake level began to rise in the early Holocene and then declined	Liu et al. (2008b)
	30	Cuona lake	91.47°E	32.03°N	The lake level began to rise in the early Holocene and then declined	Wu et al. (2005)
	31	Chen Co	90.52°E	28.85°N	The lake level began to rise in the early Holocene and then declined	Zhu et al. (2009)
	32	Bankog Co	89.57°E	31.75°N	The lake level began to decline since the early Holocene	Zhao et al. (2011)
	33	Siling Co	89°E	31.8°N	The lake level began to rise in the early Holocene and then declined	Li et al. (2009)
	34	Paiku Co	85.58°E	28.78°N	The lake level began to decline since the early Holocene	Bian et al. (2013)
	35	Bangong Co	79.42°E	33.77°N	The lake level began to rise in the early Holocene and then declined	Rossit et al. (1996)

lake level at the late Holocene, whereas increasing lake level is found in Yunnan-Guizhou plateau during the late Holocene (Table 1). The high level of modeled lake in southern China appeared not only in the early Holocene but also around the late Holocene (Figure 3b1). For northern Central Asia, a majority of lakes in eastern region are located in the

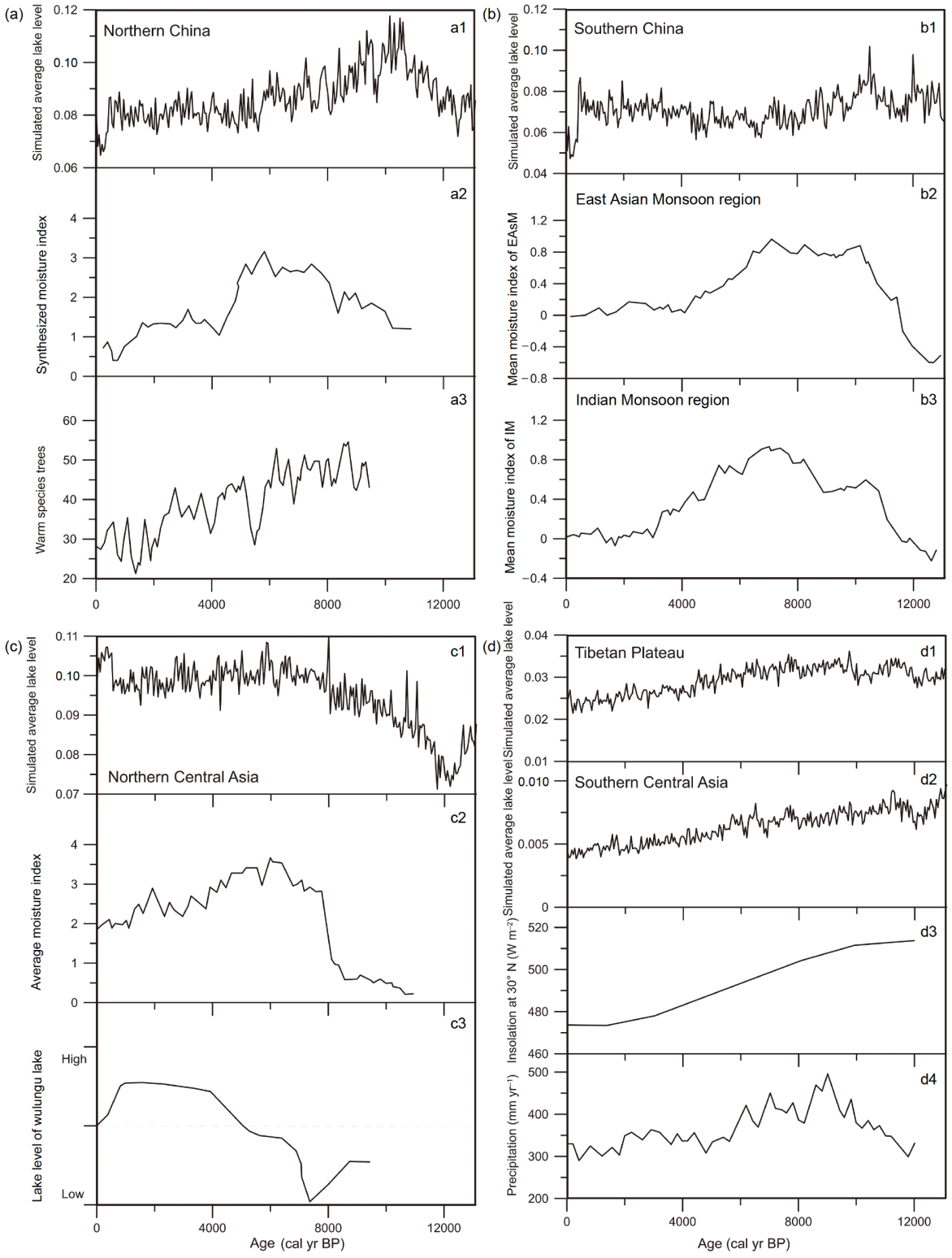

Figure 3 Comparison between simulated average lake level in different regions and paleoclimate records during the Holocene. (a1) Simulated average lake level in northern China. (a2) Pollen-based moisture index synthesized from the East Asian summer monsoon rainfall belt over northern China (Wang and Feng, 2013). (a3) Warm deciduous broad-leaved trees from Jingbo Lake in the northern China (Li et al., 2011). (b1) Simulated average lake level in southern China. (b2) and (b3) Moisture indexes from regions of East Asian summer monsoon and Indian monsoon based on continental paleo-moisture records in the Eastern Hemisphere (Wang et al., 2017). (c1) Simulated average lake level in northern Central Asia. (c2) Average moisture index calculated from lake records in the arid Central Asia (An and Chen, 2009). (c3) Lake level fluctuation derived from grain-size and pollen data from Wulungu Lake (Liu et al., 2008a). (d1) Simulated average lake level in the Tibetan Plateau. (d2) Simulated average lake level in southern Central Asia. (d3) Summer solar insolation at 30°N during the Holocene (Berger and Loutre, 1991). (d4) Reconstructed Holocene precipitation on the Tibetan Plateau (Hou et al., 2012). The corresponding curve for all descriptions is from top to bottom.

monsoon marginal zone, which experience higher lake level during the mid-Holocene. However, lake levels in western region are influenced by the westerly, and experience the higher lake level in the late Holocene (Table 1). The models reveal a rising trend of moisture in most northern Central Asia (Figure 3c1). In the Tibetan Plateau, higher lake level in records and simulations occurs during the early and mid-Holocene with declining trend throughout the Holocene, and the changing pattern shows a similar trend with that in southern Central Asia (Figure 3d1 and 3d2), indicating a gradually drying climate. However, there are few quantitative or qualitative studies on reconstruction of lake level in southern Central Asia, which is an obstacle to our verification of the simulations. Based on the simulated average lake level, it is preliminarily speculated that lake level changes in southern Central Asia are consistent with that in the Tibetan Plateau during the Holocene.

Paleoclimate records were also collected to verify whether virtual lake level varies with climate. The principle of selected records is that records can represent the average climate change of the entire region as far as possible. In northern China (Figure 3a2 and 3a3), the major trend of the average lake level in middle and late Holocene is a gradual decrease that is consistent with moisture index. Many stalagmite and lake records in southern China have been used to reveal the strength of the Asian monsoon and climatic variability of temperature and humidity. Accordingly, Asian monsoon plays an important role in influencing moisture change in southern China. Thus, we selected moisture indexes from regions of East Asian summer monsoon and Indian monsoon based on continental paleo-moisture records to compare them with the average simulated lake level, and the results show that the wettest period corresponds to the period when the lake level is highest (Figure 3b2 and 3b3). However, the simulated lake level changes in southern China (Figure 3b1) do not represent the east Asian monsoon changes, and the relationship between them should be further researched. In northern Central Asia (Figure 3c2 and 3c3), the moisture index is closely comparable to lake level change simulated by the models, showing an upward trend in the late Holocene. The simulations and records in the Tibetan Plateau match each other exactly, and they exhibit a similar changing pattern (Figure 3d3 and 3d4).

3.2 Comparison between simulated virtual lake level changes and paleoclimate records

Based on the above partition, we selected typical lakes in different regions and compared the simulated virtual lake level with climatic indicators to verify the feasibility and accuracy of the models. In northern China (Figure 4), there are many inland lakes formed in the early Holocene mainly influenced by the Asian monsoon. We simulated the lake level of Erlongwan Maar lake, Hulun lake, and Daihai lake located from east to west in northern China, and each of them has continuous paleoenvironment records. Simulations of Hulun lake are in a steady uptrend with no larger fluctuations. Decreased $\delta^{18}O$ values and negative $\delta^{13}C$ values be-

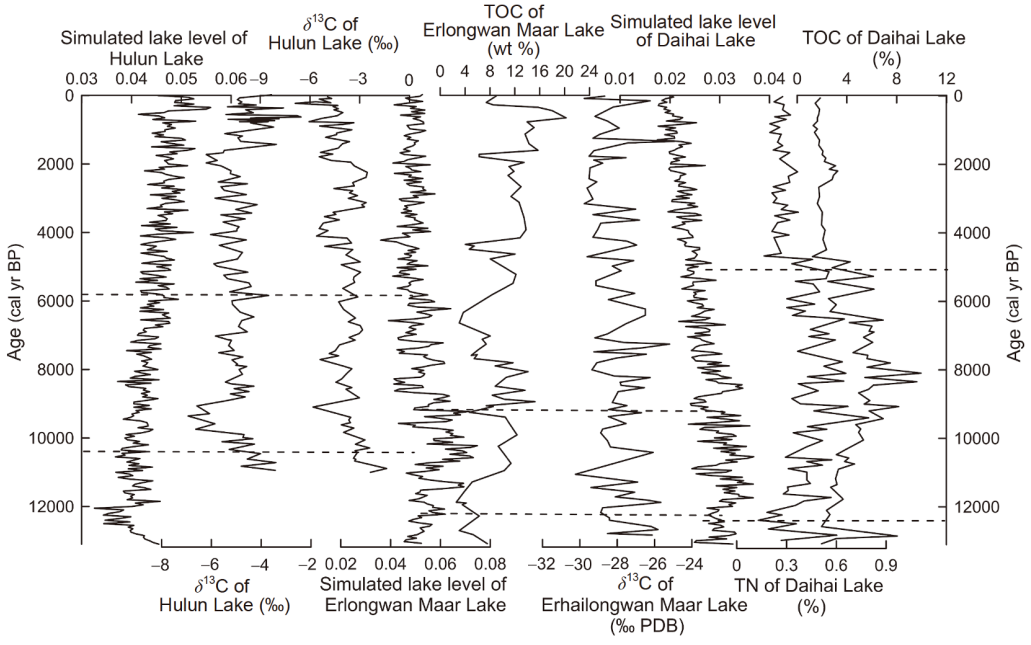

Figure 4 A comparison between typical simulated lake level and paleoclimate records in northern China during the Holocene. The corresponding curves from left to right are: simulated lake level of Hulun lake; $\delta^{18}O$ and $\delta^{13}C$ of Hulun lake came from Zhai et al. (2011); simulated lake level of Erlongwan Maar lake; TOC and $\delta^{13}C$ of Erlongwan Maar lake derived from You and Liu (2012); simulated lake level of Daihai lake; TN and TOC of Daihai lake derived from Sun et al. (2010).

tween 10000 and 6000 cal yr BP reflect a high lake level. In addition, the lake level has risen significantly during 3350–1190 cal yr BP. Simulations of Erlongwan Maar lake perform well and correspond to paleoclimate records, and both of them show a humid environment in the early Holocene. The optimal climatic conditions are conducive to the accumulation of TOC and TN, which can indirectly reflect environmental information. Higher lake level in Daihai during the early and mid-Holocene has good consistency with fluctuations in TOC and TN.

For southern China, no large lakes existed in the middle and low reaches of Yangtze River during the early Holocene, and only a few small lakes such as Gucheng lake (Jiangsu Province) were presented (Shen, 2013). Therefore, we chose Xingyun, Erhai and Dianchi lake, which were formed earlier and had continuous evolution process, to analyze the variation of lake level (Figure 5). As a result of Younger Dryas event, the three simulations show a low lake level during 13100–12000 cal yr BP. After that, the climate warms up, Dianchi and Erhai begin to expand with raised level during the early Holocene, and then decrease slowly during the mid-Holocene. And then, lake levels gradually rise during 4000 cal yr BP–present. Besides, the positive (negative) δ^{13}C values represent a relatively arid (humid) environment. According to the fluctuation of the indicators and lake level, the records are consistent with simulations shown in Figure 5. However, lake level of Xingyun does not fluctuate too much, and it declines stably from the early Holocene to late Holocene, which has a similar pattern with the variation of environment indicated by δ^{18}O values.

Taking into account the regional characteristics of the Tibetan Plateau, comparative analysis was carried out on three lakes located from east to west plateau with continuous paleoclimate records: Chen Co, Siling Co and Bangong Co (Figure 6). The climate indicators are consistent with those used in previous sections. Lake level changes of the three lakes have a similar trend which has a clear rise tendency between 12000 and 6000 cal yr BP. Then the lake level begins to decline gradually during 6000–2000 cal yr BP and has an upward trend in the modern times. The curves of paleoclimate indicator and simulated lake level in Chen Co have good consistency in fluctuation, indicating that a relatively higher lake level between 4000 and 8000 cal yr BP is correspond to wetter climatic conditions of the mid-Holocene indicated by the TOC and TN. Low δ^{18}O and negative δ^{13}C values in Bangong Co suggest the humid environment with higher lake level during early and mid-Holocene. Although the values of simulations do not fluctuate in a large extent, the changing trends for two curves of Siling Co are the same. Humid environment with negative δ^{18}O values corresponds to the increase lake level.

In northern Central Asia, we chose three typical lakes which are Qinghai lake (monsoon marginal zone with higher elevation), Qingtu lake (located in the east) and Bosten lake (located in the midst), to explore the variations of lake level and climatic characteristic (Figure 7). Several curves of lake level and climate evidence from Qinghai lake point to a low lake level between 13000 and 11000 cal yr BP, possibly corresponding to the Younger Dryas event. And after that, regional climate warms up. For 11000–8000 cal yr BP, accompanied with warming climate conditions, the highest lake level appears. Warmer than present climate conditions

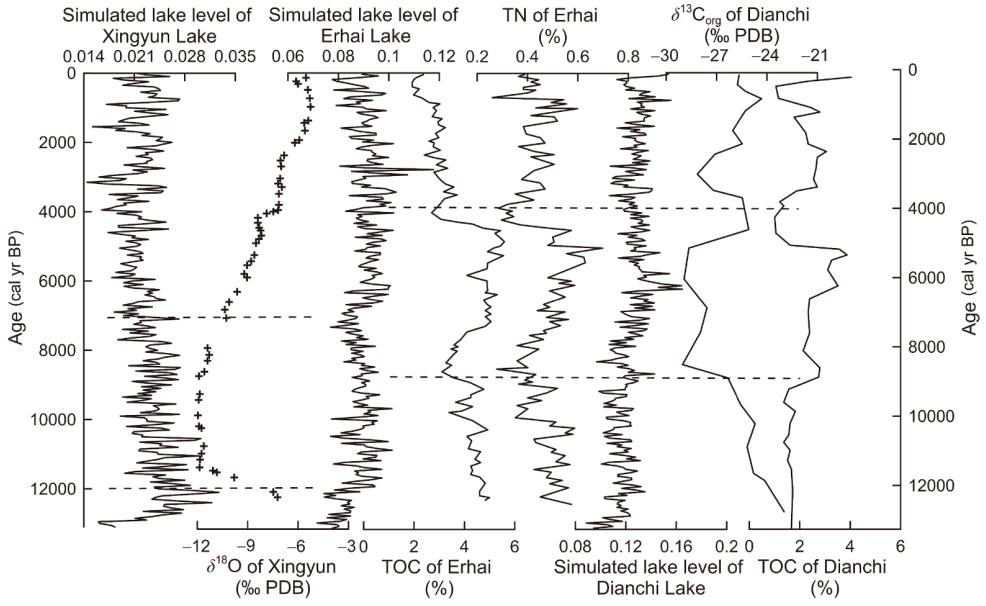

Figure 5 A comparison between typical simulated lake level and paleoclimate records in southern China during the Holocene. The corresponding curves from left to right are: simulated lake level of Xingyun lake; δ^{18}O of Xingyun lake came from Hodell et al. (1999); simulated lake level of Erhai lake; TOC and TN of Erhai lake derived from Shen et al. (2005b); simulated lake level of Dianchi lake; δ^{13}C and TOC of Dianchi lake derived from Wu et al. (1998).

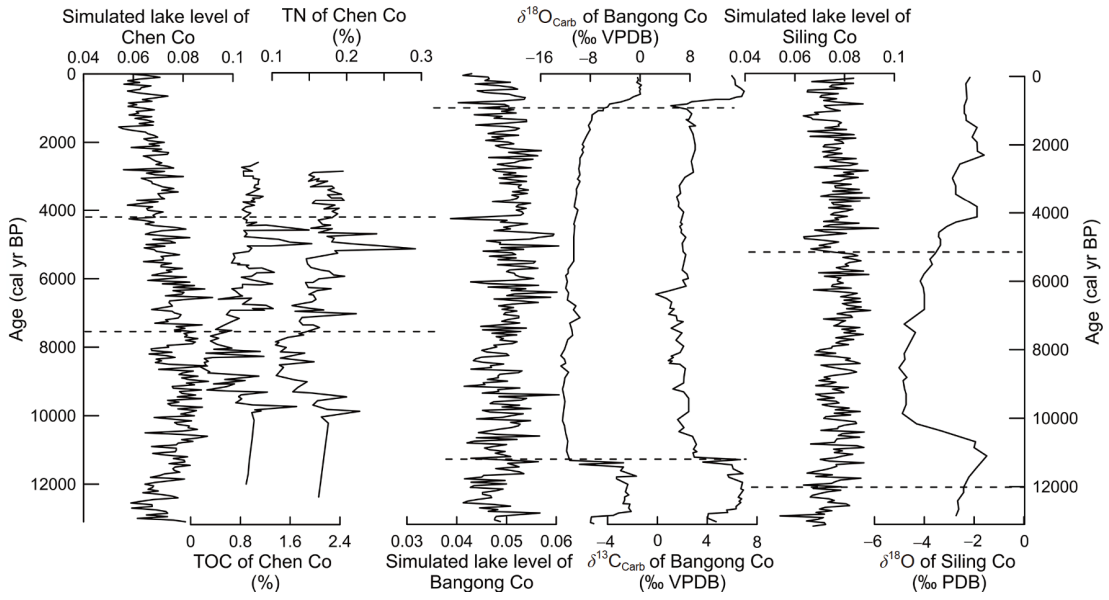

Figure 6 A comparison between typical simulated lake level and paleoclimate records in the Tibetan Plateau during the Holocene. The corresponding curves from left to right are: simulated lake level of Chen Co; TOC and TN of Chen Co came from Zhu et al. (2009); simulated lake level of Bangong Co; $\delta^{18}O$ and $\delta^{13}C$ of Bangong Co derived from Yang (2016); simulated lake level of Siling Co; $\delta^{18}O$ of Siling Co derived from Jin et al. (2016).

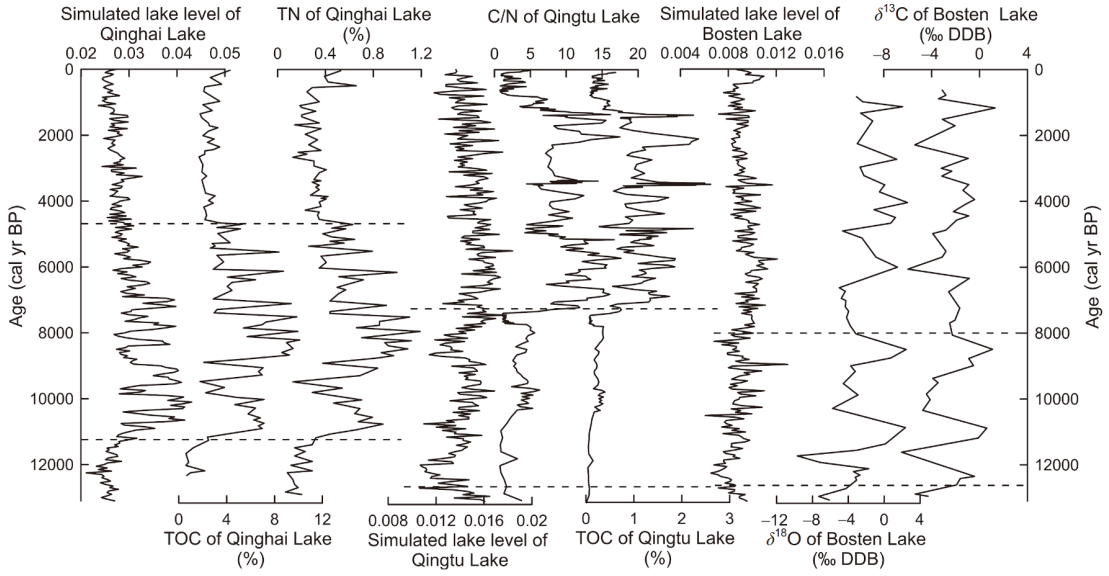

Figure 7 A comparison between typical simulated lake level and paleoclimate records in northern Central Asia during the Holocene. The corresponding curves from left to right are: simulated lake level of Qinghai lake; TOC and TN of Qinghai lake came from Shen et al. (2005a); simulated lake level of Qingtu lake; TOC and TN of Qingtu lake came from Li and Liu (2017); simulated lake level of Bosten lake; $\delta^{18}O$ of Bosten lake derived from Zhong and Xiong (1998).

terminated about 4500 cal yr BP in Qinghai lake. The simulations of Qingtu lake are also consistent with paleoclimate records. Lake level of Bosten lake has a similar trend with that in Qingtu lake, showing an obvious and slow rising trend in the mid-Holocene and then gradually decreases. The virtual lake level of Bosten lake does not show a sharp increase or decrease, but the fluctuations are consistent with climate fluctuations.

4. Discussion

As mentioned above, the climate in East and Central Asia is affected by circulation systems of the westerly winds, the Indian monsoon and the East Asian monsoon (An and Chen, 2009; Mishra et al., 2015). And the meteorological elements including precipitation, evaporation, runoff and others controlled by the circulation system are varied in different

geographical regions (Morrill, 2004). Using the approach outlined in Section 2.4, we then considered which element plays a decisive role in determining regional water balance change, and discussed the driving mechanisms determining effective moisture fluctuations in the whole study area. By applying the spatial-temporal decomposition in simulations of virtual lake level, the spatial distribution and time series of the first mode were obtained, which has contribution rate of 42%. From Figure 8, the most prominent region is northern China, Tibetan Plateau and southern Central Asia. Combing the spatial distribution with time series, the most prominent area is the same as the area where precipitation decreases (Figures 9a, 10a, 10d, 10e). And the time series of the first mode, precipitation in most areas and summer solar insolation show regionally coherent patterns of changes during the Holocene. The relationship between precipitation and summer solar radiation is worth considering. A long-term trend of stalagmite δ^{18}O records in Oman generally follows the summer insolation, suggesting that after approximately 8000 cal yr BP, monsoon precipitation decreases gradually in response to Northern Hemisphere summer solar insolation (Fleitmann et al., 2003; Wang et al., 2005). Accordingly, it is preliminarily speculated that precipitation generally follows variations in summer solar insolation during the Holocene.

According to our simulated results, we confirmed that the reasons for effective moisture changes varied with meteorological factors that changed in different regions. In northern China, especially in northeast China, reduced effective moisture through the Holocene is generally due to the combined effects of low precipitation caused by reductions in summer solar insolation, and high lake evaporation caused by increasing temperature, atmospheric radiation and shortwave radiation (Figures 9 and 10). And in Figure 9c, it is shown that enhancement of evaporation in northeast China is the most intense, which can be inferred that evaporation has a great impact on effective moisture than precipitation. In southern China, precipitation and evaporation have a trend of gradually increasing during the Holocene. Lakes which are located in coastal regions are more likely maintained by high coastal precipitation in the late Holocene (Figures 9 and 10). For northern Central Asia, the rise in effective moisture during the Holocene is due to an increase in precipitation, and a decrease in evaporation. Although the temperature also shows an increasing trend, precipitation is the main factor affecting the moisture change in this area, which might be caused by the enhancement of the westerly winds (Figures 9 and 10). However, the Tibetan Plateau and southern Central Asia have opposite trends with northern Central Asia, which is mainly reflected in precipitation and evaporation changes (Figures 9 and 10). This phenomenon indicates that the driving mechanisms of regional moisture fluctuations might be mainly controlled by the variation of Asian monsoon induced by summer solar insolation, and are different from that in northern Central Asia. These results are an important reminder that the lake water balance is not only controlled by the dominant circulation systems of the westerly winds, the Indian monsoon, and the East Asian monsoon, and it is important to consider regional characteristics of meteorological factors.

Based on the characteristics of the transient climate evolution experiment, the virtual lake level we simulated is completely water balance evolution process in the natural state, without human activities involved. Most indicators of paleoclimate change are affected by human activities in the late Holocene (Zong et al., 2010). Therefore, the verification of effective moisture change by paleoclimate records should be dominated by the early and mid-Holocene. Li and Morrill (2010) suggested that relatively high lake levels at 8.5 kyr and 6.0 kyr in the monsoon region were caused by the combined effects of low lake evaporation and high precipitation relative to the late Holocene, and increasing pre-

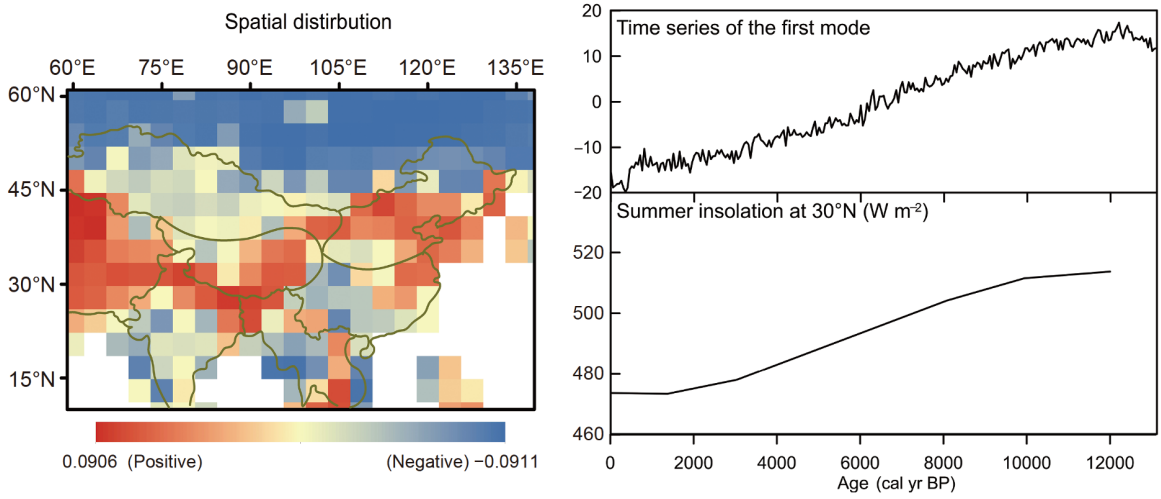

Figure 8 Spatial distribution and time series of the first mode. Red (blue, yellow) colors indicate that the influence factors of lakes in this region are positively (negative, not) correlated with solar insolation.

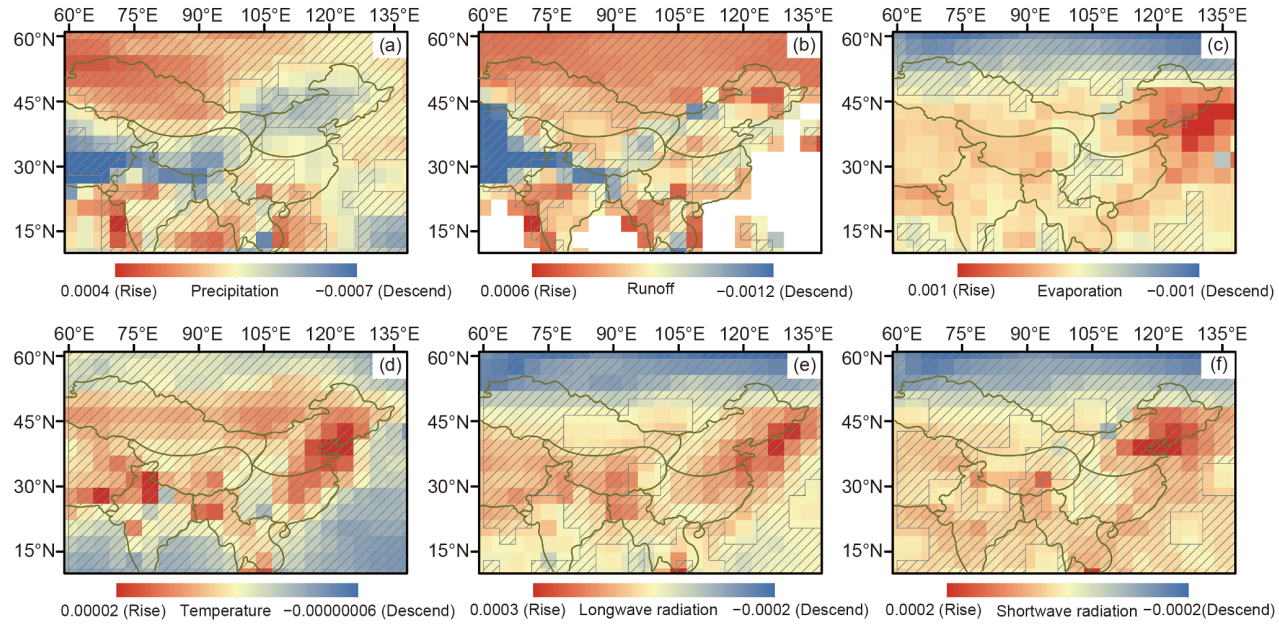

Figure 9 Trends of precipitation, runoff, evaporation, temperature, longwave radiation and shortwave radiation during the Holocene. Red (blue) colors indicate the rise (descend) in meteorological elements during the Holocene. Yellow colors indicate that there is no significant change in this area. Striping indicates the significance test is over 95%.

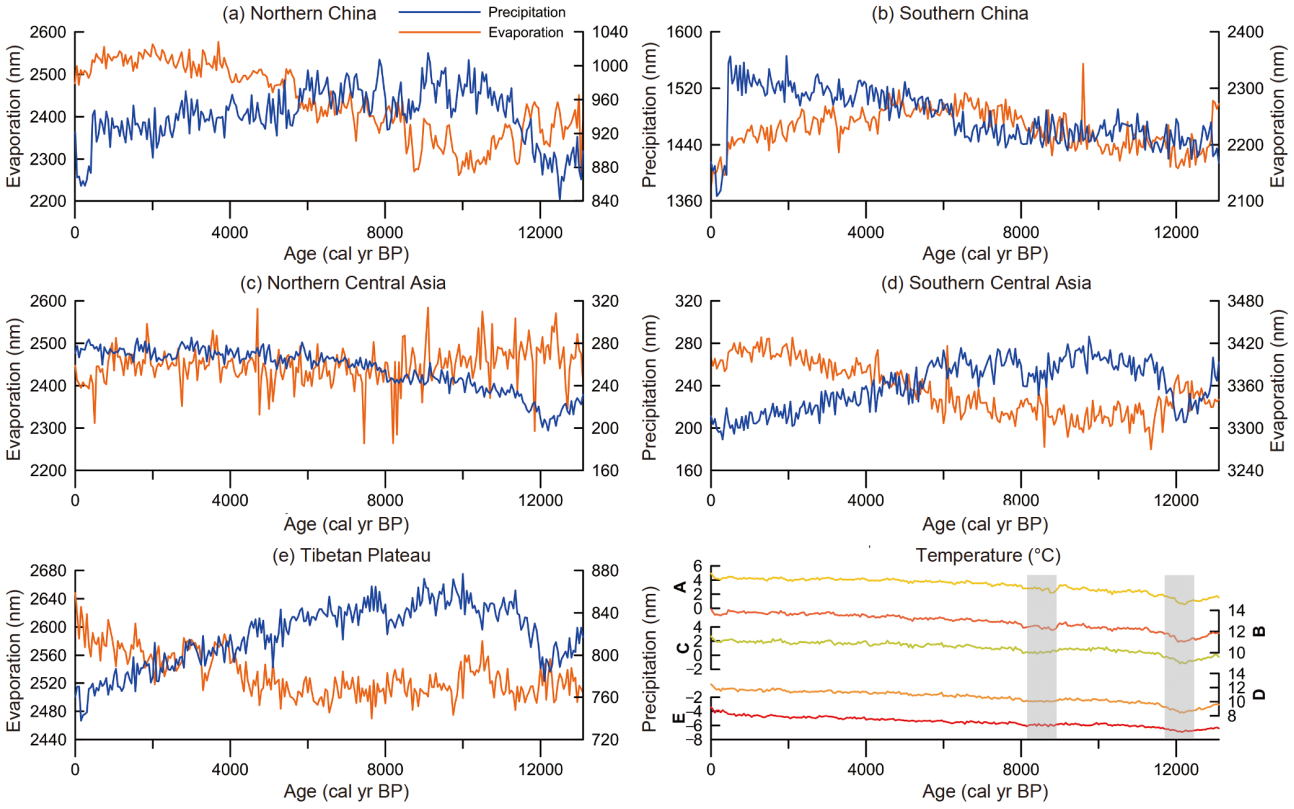

Figure 10 Time series of regional averaged temperature, precipitation and evaporation during the Holocene.

cipitation from the early to mid-Holocene maintained high lake levels in most of arid Central Asia. However, one new result of our study is that the combined effects of increasing lake evaporation and decreasing precipitation influence the decline virtual lake level in most monsoon regions with the exception of coastal regions on the millennial scale, whereas increasing precipitation determines the change of virtual lake level on the millennial scale in northern Central Asia.

Comparing with previous results, our conclusions also demonstrated that evaporation and precipitation, responsible for regional effective moisture change, vary by region and through time.

In addition, the temperature shows an upward trend in all regions (northern China, southern China, northern Central Asia, southern Central Asia and Tibetan Plateau) (Figure 10f). It shows cooling associated with the Younger Dryas, followed by Holocene warming, but also a brief cooling episode from 8500–8000 cal yr BP which was called "8.2 kyr"event caused by freshwater forcing and associated with a weakening of the Atlantic Meridional Overturning Circulation (Yan and Liu, 2019). We emphasized that the simulated trend of global temperature rise during the Holocene does not represent the actual trend of this period. Simultaneously, the precipitation (evaporation) with an overall decline (rising) trend decreases (increases) abruptly during the Younger Dryas and "8.2 kyr" cooling episodes. This pattern is similar to characteristics of northern hemisphere climate change during the Holocene (Ning et al., 2019). Our findings not only proved the sensitivity of effective moisture fluctuations to climate variability and meteorological elements change, but also proposed a new method to comprehensively understand the driving mechanisms of effective moisture change on the millennial scale.

5. Conclusion

Based on a series of lake models, we performed a continuous simulation of hypothetical lake level change to track the variability of regional effective moisture during the Holocene in East and Central Asia, and examined the driving mechanisms for water balance change in different geographical regions. Lake energy and water balance models forced by a coupled atmosphere-ocean general circulation model indicate that effective moisture gradually reduced during Holocene in northern China, southern China (with the exception of coastal regions, where the late Holocene high lake level was maintained by high coastal precipitation, possibly resulted from changes in local ocean feedbacks), Tibetan Plateau and southern Central Asia. However, variability of effective moisture during the Holocene in northern Central Asia has two changing patterns: higher moisture occurred during the early and mid-Holocene in monsoon marginal zone and higher moisture appeared during the late Holocene in the westerlies. For the most part, this agrees with moisture proxy evidence. Besides, we also concluded that decreased effective moisture in northern China was influenced by the combined effects of high lake evaporation and low precipitation. A decline in effective moisture through the Holocene in the Tibetan Plateau and southern Central Asia was primarily a result of decreased precipitation caused by the weaken of the Asian summer monsoon. Increased precipitation contributed to the effective moisture rise in northern Central Asia, which was induced by the strengthen of the westerly wind circulation.

Acknowledgements *This work was supported by the National Natural Science Foundation of China (Grant No. 41822708), the Strategic Priority Research Program of Chinese Academy of Sciences (Grant No. XDA20100102), the Second Tibetan Plateau Scientific Expedition and Research Program (STEP) (Grant No. 2019QZKK0202).*

References

An C B, Chen F H. 2009. The pattern of Holocene climate change in the arid central Asia: A case study based on lakes. J Lake Sci, 21: 329–334
Anderson L, Abbott M B, Finney B P, Edwards M E. 2005. Palaeohydrology of the Southwest Yukon Territory, Canada, based on multiproxy analyses of lake sediment cores from a depth transect. Holocene, 15: 1172–1183
Anderson L, Finney B P, Shapley M D. 2011. Lake carbonate-δ^{18}O records from the Yukon Territory, Canada: Little Ice Age moisture variability and patterns. Quat Sci Rev, 30: 887–898
Benson L V, Paillet F L. 1989. The use of total lake-surface area as an indicator of climatic change: Examples from the Lahontan Basin. Quat Res, 32: 262–275
Berger A L. 1978. Long-term variations of caloric insolation resulting from the Earth's orbital elements. Quat Res, 9: 139–167
Berger A, Loutre M F. 1991. Insolation values for the climate of the last 10 million years. Quat Sci Rev, 10: 297–317
Bian Y M, Yu J, Shao Z G, Han J E, He C G. 2013. Palynological assemblages in the Paiku Co basin of Tibet since late pleistocene and their paleoclimatic significance (in Chinese). Acta Geosci Sin, 34: 87–94
Boomer I, Aladin N, Plotnikov I, Whatley R. 2000. The palaeolimnology of the Aral Sea: A review. Quat Sci Rev, 19: 1259–1278
Brenner M, Dorsey K, Song X L, Wang Z G, Long R H, Binford M W, Whitmore T J, Moore A M. 1991. Paleolimnology of Qilu Hu, Yunnan province, China. Hydrobiologia, 214: 333–340
Chen F H, Wu W, Holmes J A, Madsen D B, Zhu Y, Jin M, Oviatt C G. 2003. A mid-Holocene drought interval as evidenced by lake desiccation in the Alashan Plateau, Inner Mongolia, China. Chin Sci Bull, 48: 1401–1410
Cheng J, Liu Z Y, He F, Otto-Bliesner B, Brady E, Lynch-Stieglitz J. 2014. Model-proxy comparison for overshoot phenomenon of Atlantic thermohaline circulation at Bølling-Allerød. Chin Sci Bull, 59: 4510–4515
Cui M L, Luo Y L, Sun X J. 2006. Paleovegetational and paleoclimatic changes in Ha'ni Lake, Jilin since 5 ka BP (in Chinese). Mar Geol Quat Geol, 26: 117–122
Davis M, Douglas C, Calcote R, Cole K L, Winkler M G, Flakne R. 2000. Holocene climate in the Western Great Lakes National Parks and Lakeshores: Implications for future climate change. Conserv Biol, 14: 968–983
Dickinson R E, Henderson-Sellers A, Kennedy P J. 1993. NCAR Technical Notes
Dickson D R, Yepsen J H, Vern Hales J. 1965. Saturated vapor pressures over Great Salt Lake brine. J Geophys Res, 70: 500–503
Ferronskii V I, Polyakov V A, Brezgunov V S, Vlasova L S, Karpychev Y A, Bobkov A F, Romaniovskii V V, Johnson T, Ricketts D, Rasmussen K. 2003. Variations in the hydrological regime of Kara-Bogaz-Gol Gulf, Lake Issyk-Kul, and the Aral Sea assessed based on data of bottom sediment studies. Water Resour, 30: 252–259
Fleitmann D, Burns S J, Mudelsee M, Neff U, Kramers J, Mangini A, Matter A. 2003. Holocene forcing of the Indian Monsoon recorded in a stalagmite from Southern Oman. Science, 300: 1737–1739
Rossit C A, Laura P A A, Bambill D, Fontes J C, Gasse F, Gibert E. 1996. Holocene environmental changes in Lake Bangong basin (Western Ti-

bet). Part 1: Chronology and stable isotopes of carbonates of a Holocene lacustrine core. Palaeogeogr Palaeoclimatol Palaeoecol, 120: 25–47
Hu G, Wang N A, Zhao Q, Cheng H Y, Chen Y S, Guo J Y. 2003. Water balance of Huahai Lake basin during a special phase (in Chinese). J Glaciol Geocryol, 25: 485–490
Hodell D A, Brenner M, Kanfoush S L, Curtis J H, Stoner J S, Song X L, Wu Y, Whitmore T J. 1999. Paleoclimate of Southwestern China for the past 50000 yr inferred from lake sediment records. Quat Res, 52: 369–380
He F. 2011. Simulating Transient Climate Evolution of the Last Deglaciation with CCSM 3. Doctoral Dissertation. Madison: University of Wisconsin
He F, Shakun J D, Clark P U, Carlson A E, Liu Z Y, Otto-Bliesner B L, Kutzbach J E. 2013. Northern Hemisphere forcing of Southern Hemisphere climate during the last deglaciation. Nature, 494: 81–85
Hou G L, E C Y, Xiao J Y. 2012. Synthetical reconstruction of the precipitation series of the Qinghai-Tibet Plateau during the Holocene (in Chinese). Prog Geogr 31: 1117–1123
Hostetler S W, Bartlein P J. 1990. Simulation of lake evaporation with application to modeling lake level variations of Harney-Malheur Lake, Oregon. Water Resour Res, 26: 2603–2612
Hostetler S W, Small E E. 1999. Response of North American freshwater lakes to simulated future climates. J Am Water Resour Assoc, 35: 1625–1637
Innes J L. 1991. High-altitude and high-latitude tree growth in relation to past, present and future global climate change. Holocene, 1: 168–173
Jiang W Y, Guo Z T, Sun X J, Wu H B, Chu G Q, Yuan B Y, Christine H, Joel G. 2006. Reconstruction of climate and vegetation changes of Lake Bayanchagan (Inner Mongolia): Holocene variability of the East Asian monsoon. Quat Res, 65: 411–420
Jie D M, Lv J F, Li Z M, Leng X T, Wang S Z, Zhang G R. 2001. Carbonate content of sedimentary core and Holocene lake-level fluctuation of Dabusu lake (in Chinese). Mar Geol Quat Geol, 21: 77–82
Jin C F, Günther F, Li S J, Jia G D, Peng P A, Gleixner G. 2016. Reduced early Holocene moisture availability inferred from δD values of sedimentary *n*-alkanes in Zigetang Co, Central Tibetan Plateau. Holocene, 26: 556–566
Joos F, Spahni R. 2008. Rates of change in natural and anthropogenic radiative forcing over the past 20000 years. Proc Natl Acad Sci USA, 105: 1425–1430
Kundu P K, Allen J S. 1976. Some three-dimensional characteristics of low-frequency current fluctuations near the Oregon coast. J Phys Oceanogr, 6: 181–199
Li C H, Wu Y H, Hou X H. 2011. Holocene vegetation and climate in Northeast China revealed from Jingbo Lake sediment. Quat Int, 229: 67–73
Li D W, Li Y K, Ma B Q, Dong G C, Wang L Q, Zhao J X. 2009. Lake-level fluctuations since the Last Glaciation in the Selin Co (Lake), Central Tibet, investigated using optically stimulated luminescence dating of beach Ridges. Environ Res Lett, 4: 1–10
Li W Y, Yao Z J. 1993. Late Quaternary Vegetation and Environment of North and Middle Subtropical Region of China (in Chinese). Beijing: China Ocean Press. 54–61
Li X Z, Liu X J, He Y X, Liu W G, Zhou X, Wang Z. 2018. Summer moisture changes in the Lake Qinghai area on the northeastern Tibetan Plateau recorded from a meadow section over the past 8400 yrs. Glob Planet Change, 161: 1–9
Li Y, Morrill C. 2010. Multiple factors causing Holocene lake-level change in monsoonal and arid central Asia as identified by model experiments. Clim Dyn, 35: 1119–1132
Li Y, Morrill C. 2013. Lake levels in Asia at the Last Glacial Maximum as indicators of hydrologic sensitivity to greenhouse gas concentrations. Quat Sci Rev, 60: 1–12
Li Y, Liu Y. 2016. The response of lake records to the circulation system and climate zones in China since the Last Glacial Maximum (in Chinese). Acta Geogr Sin, 71: 1898–1910
Li Y, Wang Y, Zhang C Q, Zhou X H, Wang N A. 2014. Changes of sedimentary facies and Holocene environments in the middle reaches of inland rivers, arid China: A case study of the Shiyang River (in Chinese). Geogr Res, 33: 1866–1880
Li Yu, Liu Y. 2017. Long-term reconstructions and simulations of the hydrological cycle in the inland rivers, arid China: A case study of the Shiyang River drainage basin (in Chinese). Adv Earth Sci, 32: 731–743
Liu X Q, Herzschuh U, Shen J, Jiang Q F, Xiao X Y. 2008a. Holocene environmental and climatic changes inferred from Wulungu Lake in northern Xinjiang, China. Quat Res, 70: 412–425
Liu X Q, Dong H L, Jason A R, Matsumoto R, Bo Y, Wang Y B. 2008b. Evolution of Chaka Salt Lake in NW China in response to climatic change during the Latest Pleistocene-Holocene. Quat Sci Rev, 27: 867–879
Liu Z Y, Otto-Bliesner B L, He F, Brady E C, Tomas R, Clark P U, Carlson A E, Lynch-Stieglitz J, Curry W, Brook E J, Erickson D, Jacob R, Kutzbach J, Cheng J. 2009. Transient simulation of last deglaciation with a new mechanism for bølling-allerød warming. Science, 325: 310–314
Luoto T P, Sarmaja-Korjonen K. 2011. Midge-inferred Holocene effective moisture fluctuations in a subarctic lake, northern Lapland. Boreas, 40: 650–659
Ma C M, Zhu C, Zheng C G, Wu C L, Guan Y, Zhao Z P, Huang L Y, Huang R. 2008. High-resolution geochemistry records of climate changes since late-glacial from Dajiuhu peat in Shennongjia Mountains, Central China. Chin Sci Bull, 53: 28–41
Madsen D B, Haizhou M, Rhode D, Brantingham P J, Forman S L. 2008. Age constraints on the Late Quaternary evolution of Qinghai Lake, Tibetan Plateau. Quat Res, 69: 316–325
Mishra P K, Anoop A, Schettler G, Prasad S, Jehangir A, Menzel P, Naumann R, Yousuf A R, Basavaiah N, Deenadayalan K, Wiesner M G, Gaye B. 2015. Reconstructed late Quaternary hydrological changes from Lake Tso Moriri, NW Himalaya. Quat Int, 371: 76–86
Morrill C. 2004. The influence of Asian summer monsoon variability on the water balance of a Tibetan lake. J Paleolimnol, 32: 273–286
Morrill C, Small E E, Sloan L C. 2001. Modeling orbital forcing of lake level change: Lake Gosiute (Eocene), North America. Glob Planet Change, 29: 57–76
Ning L, Liu J, Bradley R S, Yan M. 2019. Comparing the spatial patterns of climate change in the 9th and 5th millennia BP from TRACE-21 model simulations. Clim Past, 15: 41–52
Peltier W R. 2004. Global glacial isostasy and the surface of the ice-age Earth: The ICE-5G (VM 2) model and GRACE. Annu Rev Earth Planet Sci, 32: 111–149
Pollard D, Schulz M. 1994. A model for the potential locations of Triassic evaporite basins driven by paleoclimatic GCM simulations. Glob Planet Change, 9: 233–249
Qin B Q, Yu G. 1998. Implications of lake level variations at 6 ka and 18 ka in mainland Asia. Glob Planet Change, 18: 59–72
Rahmstorf S, Crucifix M, Ganopolski A, Goosse H, Kamenkovich I, Knutti R, Lohmann G, Marsh R, Mysak L A, Wang Z, Weaver A J. 2005. Thermohaline circulation hysteresis: A model intercomparison. Geophys Res Lett, 32: 1–5
Ricketts R D, Johnson T C, Brown E T, Rasmussen K A, Romanovsky V V. 2001. The Holocene paleolimnology of Lake Issyk-Kul, Kyrgyzstan: Trace element and stable isotope composition of ostracodes. Palaeogeogr Palaeoclimatol Palaeoecol, 176: 207–227
Sharma A, Huang H P, Zavialov P, Khan V. 2018. Impact of desiccation of Aral Sea on the regional climate of central Asia using WRF model. Pure Appl Geophys, 175: 465–478
Sevastyanov D V, Smirnova N P. 1986. Issik Kul Lake and Tendency of its Natural Development (in Russian). Leningrad: Nauka. 256
Sevastyanov D V, Dorofeyuk N I. 1992. The history of the water ecosystem of Mongolia (in Russian). Izv Vses Geogr Obshch, 124: 123–138
Shen J. 2013. Spatiotemporal variations of Chinese lakes and their driving mechanisms since the Last Glacial Maximum: A review and synthesis of lacustrine sediment archives. Chin Sci Bull, 58: 17–31
Shen J, Liu X Q, Wang S M, Matsumotob R. 2005a. Palaeoclimatic changes in the Qinghai Lake area during the last 18000 years. Quat Int, 136: 131–140
Shen J, Wu R J, An Z S. 1998. Characters of the organic δ^{13}C and paleoenvironment in the section of Dabusu Lake (in Chinese). J Lake Sci, 10: 8–10

Shen J, Yang L Y, Yang X D, Matsumoto R, Tong G B, Zhu Y X, Zhang Z K, Wang S M. 2005b. Lake sediment records on climate change and human activities since the Holocene in Erhai catchment, Yunnan Province, China. Sci China Ser D-Earth Sci, 48: 353–363
Stommel H. 1961. Thermohaline convection with two stable regimes of flow. Tellus, 13: 224–230
Sun Q L, Wang S M, Zhou J, Cheng Z Y, Shen J, Xie X P, Wu F, Chen P. 2010. Sediment geochemistry of Lake Daihai, north-central China: Implications for catchment weathering and climate change during the Holocene. J Paleolimnol, 43: 75–87
Sun Q L, Wang S M, Zhou J, Shen J, Chen P, Xie X P, Wu F. 2009. Lake surface fluctuations since the late glaciation at Lake Daihai, North central China: A direct indicator of hydrological process response to East Asian monsoon climate. Quat Int, 194: 45–54
Tang L Y. 1992. Vegetation and climate history at Menghai, Yunnan during the past 42000 years (in Chinese). Acta Micropalaeontol Sin, 9: 433–455
Tarasov P E, Kremenetskii K V. 1995. Geochronology and stratigraphy of the Holocene lacustrine-bog deposits in northern and central Kazakhstan. Stratigr Geol Correl, 3: 73–80
Wang L, Rioual P, Panizzo V N, Lu H Y, Gu Z Y, Chu G Q, Yang D G, Han J T, Liu J Q, Mackay A W. 2012. A 1000-yr record of environmental change in NE China indicated by diatom assemblages from maar lake Erlongwan. Quat Res, 78: 24–34
Wang W, Feng Z D. 2013. Holocene moisture evolution across the Mongolian Plateau and its surrounding areas: A synthesis of climatic records. Earth-Sci Rev, 122: 38–57
Wang W, Feng Z D, Ran M, Zhang C J. 2013. Holocene climate and vegetation changes inferred from pollen records of lake Aibi, northern Xinjiang, China: A potential contribution to understanding of Holocene climate pattern in East-central Asia. Quat Int, 311: 54–62
Wang Y B, Bekeschus B, Handorf D, Liu X Q, Dallmeyer A, Herzschuh U. 2017. Coherent tropical-subtropical Holocene see-saw moisture patterns in the Eastern Hemisphere monsoon systems. Quat Sci Rev, 169: 231–242
Wang Y, Cheng H, Edwards R L, He Y Q, Kong X G, An Z S, Wu J Y, Kelly M J, Dykoski C A, Li X D. 2005. The Holocene Asian Monsoon: Links to solar changes and North Atlantic climate. Science, 308: 854–857
Weare B C, Newell R E. 1977. Empirical orthogonal analysis of atlantic ocean surface temperatures. Q J R Met Soc, 103: 467–478
Wen R L, Xiao J L, Chang Z G, Zhai D Y, Xu Q H, Li Y C, Itoh S, Lomtatidze Z. 2010. Holocene climate changes in the mid-high-latitude-monsoon margin reflected by the pollen record from Hulun Lake, northeastern Inner Mongolia. Quat Res, 73: 293–303
Wünnemann B, Mischke S, Chen F H. 2006. A Holocene sedimentary record from Bosten Lake, China. Palaeogeogr Palaeoclimatol Palaeoecol, 234: 223–238
Wu J, Shen J. 2010a. Paleoclimate evolution since 27.7 ka BP reflected by grain size variation of a sediment core from Lake Xingkai, northeastern Asia (in Chinese). J Lake Sci, 22: 110–118
Wu J, Shen J. 2010b. Paleoenviromental and paleoclimatic changes in Lake Xingkai inferred from stable carbon and nitrogen isotopes of bulk organic matter since 28 ka BP (in Chinese). Acta Sedimentol Sin, 28: 365–372
Wu X D, Zhang Z H, Xu X M, Shen J. 2012. Asian summer monsoonal variations during the Holocene revealed by Huguangyan maar lake sediment record. Palaeogeogr Palaeoclimatol Palaeoecol, 323-325: 13–21
Wu Y H, Wu R J, Xue B, Qian J L, Xiao J Y. 1998. Paleoenvironmental Evolution in Dianchi Lake Area since 13 ka BP (in Chinese). J Lake Sci, 10: 5–9
Wu Z H, Zhao X T, Wu Z H, Hu D G, Ma Z B, Ye P S, Jiang W. 2005. Active faults and their kinematic feature at the Amdo-Tsona graben, central Xizang (in Chinese). Quat Sci, 25: 490–502
Xiao J L, Chang Z G, Wen R L, Zhai D Y, Itoh S, Lomtatidze Z. 2009. Holocene weak monsoon intervals indicated by low lake levels at Hulun Lake in the monsoonal margin region of northeastern Inner Mongolia, China. Holocene, 19: 899–908
Xiao J L, Xu Q H, Nakamura T, Yang X L, Liang W D, Inouchi Y. 2004. Holocene vegetation variation in the Daihai Lake region of north-central China: A direct indication of the Asian monsoon climatic history. Quat Sci Rev, 23: 1669–1679
Xue B, Yu G. 2010. Changes of atmospheric circulation since the last interstadial as indicated by the lake-status record in China. Acta Geol Sin-Engl Ed, 74: 836–845
Yan M, Liu J. 2019. Physical processes of cooling and mega-drought during the 4.2 ka BP event: Results from TraCE-21 ka simulations. Clim Past, 15: 265–277
Yang H J, Zhao Y Y, Liu Z Y, Li Q, He F, Zhang Q. 2015. Heat transport compensation in atmosphere and ocean over the past 22000 years. Sci Rep, 5: 16661
Yang Y P. 2016. Climate and Environment Changes recorded by sediments from Bangong Co in Tibet since last deglaciation. Dissertation for Master's Degree. Lanzhou: University of Lanzhou
Yao J Q, Chen Y N, Zhao Y, Yu X J. 2018. Hydroclimatic changes of Lake Bosten in Northwest China during the last decades. Sci Rep, 8: 9118
You H T, Liu J Q. 2012. High-resolution climate evolution derived from the sediment records of Erlongwan Maar Lake since 14 ka BP. Chin Sci Bull, 57: 3610–3616
Yu C X, Luo Y L, Sun X J. 2008. A High-resolution pollen records from Ha'ni lake, Jilin, Northern China showing climate changes between 13.1 cal ka BP and 4.5 cal ka BP (in Chinese). Quat Sci, 28: 929–938
Zhai D Y, Xiao J L, Zhou L, Wen R L, Chang Z G, Wang X, Jin X D, Pang Q Q, Itoh S. 2011. Holocene East Asian monsoon variation inferred from species assemblage and shell chemistry of the ostracodes from Hulun Lake, Inner Mongolia. Quat Res, 75: 512–522
Zhang E L, Wang Y B, Sun W W, Shen J. 2016. Holocene Asian monsoon evolution revealed by a pollen record from an alpine lake on the southeastern margin of the Qinghai-Tibetan Plateau, China. Clim Past, 12: 415–427
Zhang S R, Xiao J L, Xu Q H, Wen R L, Fan J W, Huang Y, Yamagata H. 2018. Differential response of vegetation in Hulun Lake region at the northern margin of Asian summer monsoon to extreme cold events of the last deglaciation. Quat Sci Rev, 190: 57–65
Zhang Y, Gao X, Zhong Z Y, Chen J, Peng B Z. 2009. Sediment accumulation of Dianchi Lake determined by ^{137}Cs dating. J Geogr Sci, 19: 225–238
Zhao Q, Wang N A, Li X G, Cheng H Y, Li Y, Li Gang. 2005. Environmental change around the Qingtu Lake since 9500 a BP (in Chinese). J Glaciol Geocryol, 27: 352–359
Zhao X T, Zhao Y Y, Zheng M P, Ma Z B, Cao J K, Li M H. 2011. Late Quaternary lake development and denivellation of Bankog Co as well as lake evolution of southeastern North Tibetan Plateau during the last Great Lake Period (in Chinese). Acta Geosci Sin, 32: 13–26
Zhao Y T, An C B, Mao L M, Zhao J J, Tang L Y, Zhou A F, Li H, Dong W M, Duan F T, Chen F H. 2015. Vegetation and climate history in arid western China during MIS2: New insights from pollen and grain-size data of the Balikun Lake, eastern Tien Shan. Quat Sci Rev, 126: 112–125
Zheng Y H, Pancost R D, Naafs B D A, Li Q Y, Liu Z, Yang H. 2018. Transition from a warm and dry to a cold and wet climate in NE China across the Holocene. Earth Planet Sci Lett, 493: 36–46
Zhong W, Xiong H G. 1998. Isotopic evidence for Holocene climatic changes in Bosten Lake, Southern Xinjiang, China. Chin Geogr Sci, 8: 176–182
Zhou J, Wang S M, Lv J. 2003. Climatic and enviromental changes from the sediment record of Erhai lake over the past 10000 years (in Chinese). J Lake Sci, 15: 104–111
Zhu L P, Zhen X L, Wang J B, Lv H Y, Xie M P, Kitagawa H, Possnert G. 2009. A ~30000-year record of environmental changes inferred from Lake Chen Co, Southern Tibet. J Paleolimnol, 42: 343–358
Zong Y Q, Yu F L, Huang G Q, Lioyd J M, Yim W W S. 2010. Sedimentary evidence of Late Holocene human activity in the Pearl River delta, China. Earth Surf Process Landforms, 35: 1095–1102

(Responsible editor: Xiaodong LIU)